Reaction Dynamics of Proton-Coupled Electron Transfer from Reduced ZnO Nanocrystals

Miles N. Braten,[†,‡] Daniel R. Gamelin,[†] and James M. Mayer*[,§,†,‡]

[†]Department of Chemistry, University of Washington, Seattle, Washington 98195-1700, United States and [‡]Department of Chemistry, Yale University, New Haven, Connecticut 06520-8107, United States [§]Present address: Department of Chemistry, Yale University, New Haven, CT 06520.

ABSTRACT The creation of systems that efficiently interconvert chemical and electrical energies will be aided by understanding proton-coupled electron transfers at solution—semiconductor interfaces. Steps in developing that understanding are described here through kinetic studies of reactions of photoreduced colloidal zinc oxide (ZnO) nanocrystals (NCs) with the nitroxyl radical TEMPO. These reactions proceed by proton-coupled electron transfer (PCET) to give the hydroxylamine TEMPOH. They occur on the submillisecond to seconds time scale, as monitored by stopped-flow optical spectroscopy. Under conditions of excess TEMPO, the reactions are multiexponential in character. One of the contributors to this multiexponential kinetics may be a distribution of reactive proton sites. A graphical overlay method shows the reaction to be first order in [TEMPO]. Different electron concentrations in otherwise identical NC samples were achieved by three different methods: differing photolysis times, premixing with an unphotolyzed sample, or prereaction with TEMPO. The reaction velocities were consistently higher for NCs with higher numbers of electrons. For instance, NCs with an average of 2.6 e^-/NC reacted faster than otherwise identical samples containing $\leq$1 e^-/NC. Surprisingly, NC samples with the same average number of electrons but prepared in different ways often had different reaction profiles. These results show that properties beyond electron content determine PCET reactivity of the particles.

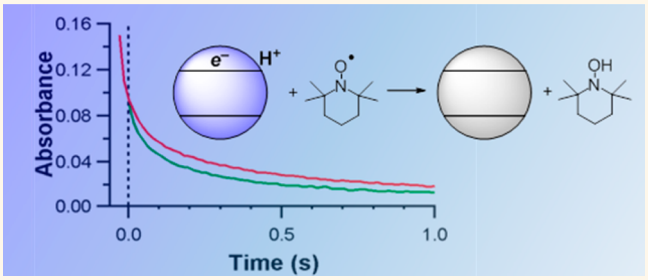

KEYWORDS: zinc oxide · proton-coupled electron transfer · multiexponential kinetics · stopped-flow kinetics · protons · TEMPO

Many of the critical energy conversion reactions being studied at semiconductor interfaces, such as the oxidations of water and H_2, and the reductions of protons and CO_2, are inherently proton-coupled electron transfer (PCET) processes. These reactions are typically described as charge transfer (CT) processes, and their dynamics and mechanisms are usually discussed primarily in terms of the electronic energies of the charge carriers.[1−5] Other factors have been identified, including the nature and density of the surface ligands[6,7] and the crystal plane exposed to the solution.[8] However, there has been little study of the role of the protons in the kinetics of these reactions, outside of the typical Nernstian dependence of the band energies on proton activity (pH).[9,10]

Previous work from our laboratory has demonstrated that photoreduced colloidal zinc oxide (ZnO) and titanium dioxide (TiO_2) nanocrystals (NCs) can react by proton-coupled electron transfer with organic hydrogen atom acceptors.[11] The presence of chemically active protons is indicated by a number of observations, including the formation of protonated reaction products in aprotic media. Thermodynamic coupling of the protons and electrons in ZnO NCs was observed through electron transfer from one-electron reductants to the NCs upon addition of protons to suspensions of ZnO nanocrystals in aprotic solvents.[12]

This report is focused on the kinetics of the PCET reaction of photoreduced ZnO NCs with the nitroxyl radical TEMPO, which forms the hydroxylamine TEMPOH (2,2,6,6-tetramethyl-piperidin-1-yl-oxyl *to* *N*-hydroxy-2,2,6,6-tetramethylpiperidine), eq 1. To write a balanced chemical equation, we write the photoreduced ZnO NCs as ZnO: e^-_{CB}/H^+. The subscript CB indicates that the electrons in these ZnO NCs occupy conduction band (CB)-like orbitals that are delocalized over the entire NC.[13] The presence of

* Address correspondence to james.mayer@yale.edu.

Received for review July 8, 2015 and accepted September 15, 2015.

Published online September 15, 2015
10.1021/acsnano.5b04222

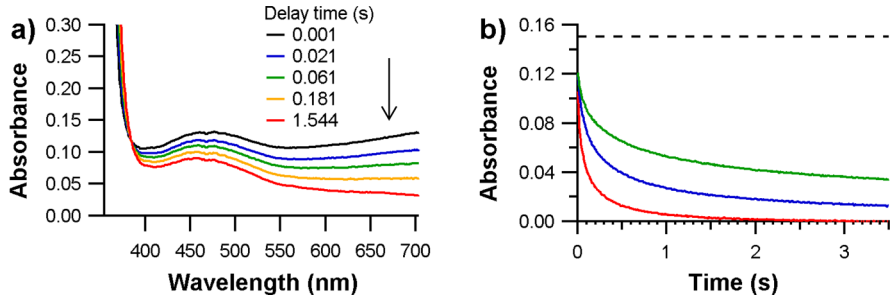

Figure 1. Absorption spectra and extracted single wavelength data showing the reaction of reduced ZnO NCs (0.17 mM, [e^-] = 0.24 mM) with TEMPO. (a) Stacked spectra from 1 ms to 1.54 s from reaction of reduced NCs with 4.8 mM TEMPO, black arrow indicating direction of absorbance change with time. The broad peak at 460 nm is due to TEMPO. (b) Absorbance at 700 nm plotted over 3.5 s for [TEMPO] = 0.24 mM (green, top), 1.2 mM (blue, middle), and 4.8 mM (red, bottom). The black dashed line represents the initial absorbance if no reaction had occurred, determined from half of the absorbance of a spectrum of reduced, unreacted NCs pushed into the mixing chamber of the stopped-flow.

CB electrons is indicated by the blue color of the NC suspension, so in eq 1 the circle representing the reduced NCs is colored blue.

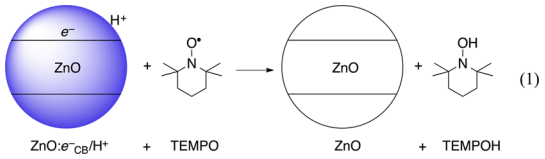

Most CT studies of NCs have examined photochemical or photoinitiated processes limited to short-lived photoexcited states [for some exceptions, see[9,10,14−16]]. This work uses stopped-flow spectroscopy to study the PCET reactivity of stable reduced NC suspensions. These reactions are slow, occurring on a milliseconds-to-seconds time scale, and are relevant to PCET catalysis at oxide interfaces. These TEMPO reactions are slower than the more typically studied photoinduced electron transfer (ET) processes in part because of their lower driving force. PCET reactions that are more exoergic can proceed much more quickly, such as the reaction of photogenerated ZnO:e^-_{CB}/H^+ with the 2,4,6-tri-*tert*-butylphenoxyl radical ($^tBu_3ArO^•$), which has a 0.5 eV larger driving force and occurs with $k \sim 10^7$ M^{-1} s^{-1}.[11] This example suggests that the involvement of proton transfer does not necessarily make the reactions slow. The slow time scale and proton-coupled nature of these reactions make them interesting models for steps occurring in fuel cell or solar fuel production, as these processes also occur on relatively slow time scales.[17]

Reproducible kinetic data for e^-/H^+ transfer from reduced ZnO to TEMPO have been obtained, by comparing aliquots from the same suspension of NCs. The disappearance of the CB electrons is multiexponential but the kinetics are simple first-order in [TEMPO]. Using aliquots from a single batch of NCs, we have prepared sets of reduced ZnO suspensions that are compositionally essentially identical *via* slightly different chemical routes. Despite having essentially the same average numbers of electrons, protons and capping ligands, and the same electronic spectra, these samples show different kinetic behavior with TEMPO. The results show that electronic properties are not sufficient to understand colloidal semiconductor charge transfer reactions. We tentatively suggest that the history of the NC solution may yield different populations of protons that play a role beyond modulating the energetics, and we suggest that the protons need to be explicitly considered when X−H bonds are being formed or cleaved.

RESULTS AND DISCUSSION

A. Description of Kinetic Behavior. Mixing reduced ZnO NC colloids with anaerobic solutions of TEMPO causes rapid loss of the broad low-energy absorbance of the ZnO:e^-_{CB}/H^+ (Figure 1a). Since TEMPOH is the product, this reaction involves the transfer of one e^-_{CB} and one H^+ to the substrate.[11] Reactions were typically carried out under conditions of excess TEMPO, with the e^-_{CB} as the limiting reagent, and were monitored *via* the absorbance at 700 nm, which scales linearly with the concentration of e^-_{CB}.[11,12] The decay in the TEMPO absorbance (λ_{max} 460 nm) is consistent with the changes at 700 nm. Control experiments reacting uncharged ZnO NCs with TEMPO did not show any reaction, as would have been evident from a decrease in the TEMPO optical absorbance. The colloidal ZnO:e^-_{CB}/H^+ are similarly stable for extended periods.

In the first set of experiments, reactions were monitored for one sample of reduced ZnO NCs with three different concentrations of TEMPO (Figure 1b). As described in the Experimental Section, all of the experiments reported here used this kind of comparison, starting from a single batch of NCs, to ensure that their properties were identical for all of the kinetic runs within a comparative set. In all of the kinetic runs, the absorbance at 700 nm at the first time point (1 ms) was significantly below the true initial value, calculated by halving the averaged absorbance of the reduced NC solution alone in the observation cell (without TEMPO). The absorbance values were obtained before and after reactions with TEMPO had been monitored by flushing through 0.5−1.0 mL of the reduced NC solution.

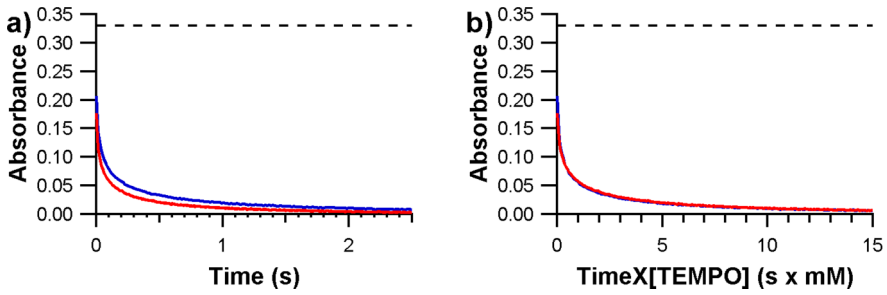

Figure 2. Reaction of reduced ZnO ([NC] = 0.17 mM; [e^-] = 0.47 mM) and TEMPO (blue line = 4.8 mM; red line = 9.6 mM). (a) Absorbance at 700 nm plotted for reactions with two concentrations of TEMPO; the red trace with the higher concentration of substrate decays faster. (b) The data on the left plotted with the time axis multiplied by the [TEMPO]; the traces overlay indicating a first-order dependence on [TEMPO]. Dashed lines indicate the expected initial absorbance if no reaction occurred, obtained from half of the absorbance of a spectrum of reduced, unreacted NCs in the stopped-flow.

Scheme 1. Manipulation of NCs Solutions To Observe Effects on Reaction Dynamics of Photoreduced ZnO NCs and TEMPO[a]

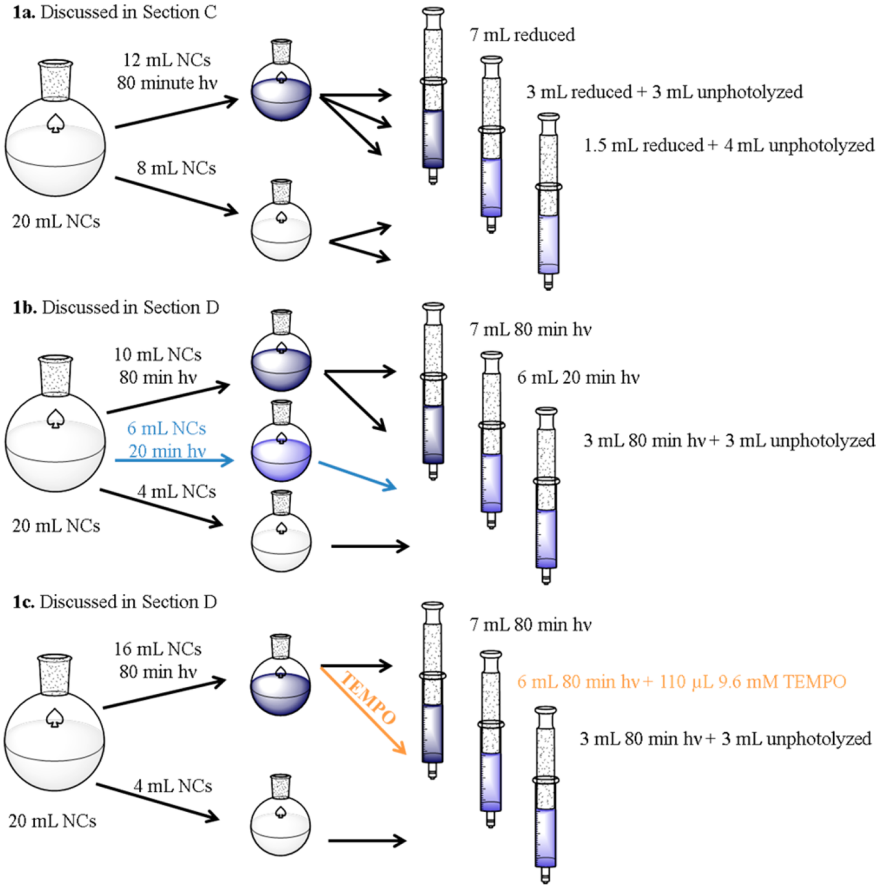

[a] Key: (a) dilution of photoreduced NCs with unphotolyzed NCs, Section C; (b) NCs with same electron content reached through short photolysis time or long photolysis time and dilution with unreduced NCs, Section D; (c) NCs with same electron content reached though oxidation with TEMPO or dilution with unreduced NCs, Section D.

In Figure 1b and some of the other figures, this initial absorbance is shown as a horizontal dotted line.

With each concentration of TEMPO, the decay in absorbance at 700 nm [A(700)] was multiexponential. For instance, in a reaction with [e^-] = 0.24 mM and [TEMPO] = 1.2 mM (blue [middle] trace in Figure 1b), 20% of the reaction is complete within the 1 ms mixing time of the instrument. It took 100 ms for the reaction to reach 50% completion and required 2 s to reach 75% completion. The decays can be fit to a stretched exponential function or (poorly) to a sum of two exponential functions, as described in the Supporting Information. In the biexponential fits, the time constants differ by roughly an order of magnitude.

B. First-Order Dependence on TEMPO Concentration. Higher concentrations of TEMPO increase the reaction velocity, as is qualitatively evident from the time traces in Figures 1b and 2a. In Figure 2, TEMPO is in 10- and

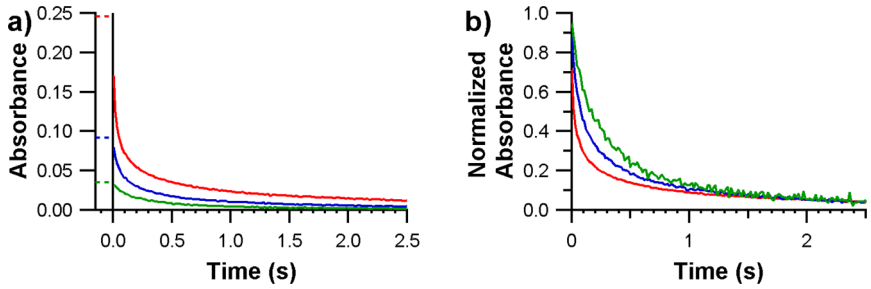

Figure 3. Plots for reaction of reduced ZnO NC solutions with TEMPO. [NC] = 0.13 mM; [e^-] = 0.35 (red, top); 0.13 (blue, middle); 0.049 mM (green, bottom); [TEMPO] = 4.8 mM. (a) Absorbance at 700 nm over the first 2.5 s of the reaction. (b) Normalized absorbance, $(A_t - A_{final})/(A_{initial} - A_{final})$ *vs t*. The dashed lines before zero indicate the expected initial absorbance for each NC aliquot if no reaction occurred, obtained from half of the absorbance of a spectrum of reduced, unreacted NCs in the stopped-flow.

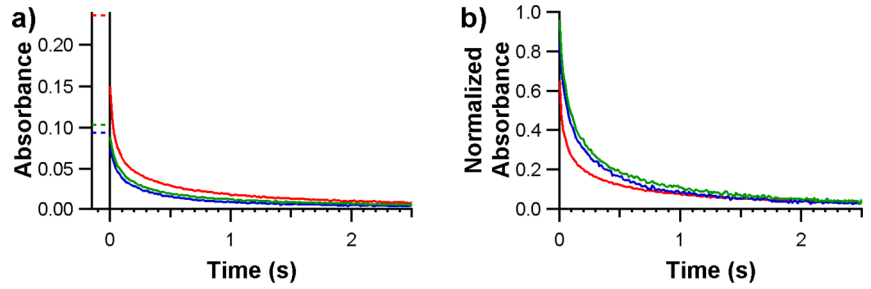

Figure 4. Kinetic plots for reactions of TEMPO with ZnO NCs ([NC] = 0.13 mM) reduced through different methods: 80 min photolysis (red), [e^-] = 0.34 mM; 80 min photolysis diluted with uncharged NCs (blue), [e^-] = 0.13; 20 min photolysis (green) [e^-] = 0.15 mM) with TEMPO (4.8 mM). (a) Absorbance at 700 nm *vs* time. (b) Normalized absorbance $(A_t - A_{final})/(A_{initial} - A_{final})$ *vs t*. The dashed lines before zero indicate the expected initial absorbance for each NC aliquot if no reaction occurred, obtained from half of the absorbance of a spectrum of reduced, unreacted NCs in the stopped-flow.

20-fold excess relative to electrons. The dependence of these reactions on the TEMPO concentration is indicated by plotting A(700) versus the product of time and [TEMPO] (Figure 2b). This scaling of the time axis causes the two traces to overlay very closely over the entire reaction. This close overlay has been observed in repeated experiments of this kind. The overlay of the kinetic traces *vs* {time × [TEMPO]} shows that the reaction is first order in [TEMPO].[18] This scaling can be viewed as a graphical definition of first-order behavior.[19]

C. Dependence on the Number of Electrons per NC. The effect of the extent of NC reduction on PCET reaction dynamics was studied by changing the electron content of different aliquots of a NC suspension. This was first done by diluting photolyzed aliquots with unphotolyzed aliquots of NCs in the glovebox, Scheme 1a. Since charge transfer between NCs is very fast,[20] these samples rapidly equilibrated to different electron concentrations. There was minor air oxidation during sample loading onto the stopped-flow instrument, so the absorbance at 700 nm was used to measure the e^- concentration for each sample. Dividing the e^- concentration by the NC concentration gives the average e^-_{CB}/NC for each solution, being 2.7, 0.9, and 0.4 in this experiment. For each sample, the reaction with 4.8 mM TEMPO displayed multiexponential A(700) *vs* time traces, qualitatively similar to those as described above (Figure 3a).

The traces can be directly compared by normalizing the data, $(A_t - A_{final})/(A_{initial} - A_{final})$ (Figure 3b; semilog plots are given in the Supporting Information), where $A_{initial}$ is the independently measured expected absorbance at t = 0 (see above). A_{final} is obtained from averaging the final 25 time points in reactions monitored to 15 s. It is qualitatively clear that the more highly reduced NCs react more quickly. For instance, the times for 50% of the electrons to react are 15, 75, and 160 ms for the 2.7, 0.9, and 0.4 e^-_{CB}/NC samples, respectively. Determining a quantitative relationship between the e^-_{CB}/NC and the kinetics has not been possible due to the complexity of the multiexponential kinetics. The origin of the multiexponential behavior is discussed below.

D. Dependence on Pathway to NC Electron Content. In the experiment described in Scheme 1b, a NC suspension was split into aliquots and reduced by three different methods. The first sample was photolyzed for 80 min, yielding NCs reduced on average by 2.6 e^-_{CB}/NC once loaded into the stopped flow. The second sample, photolyzed for 20 min, provided a solution with 1.1 e^-_{CB}/NC. The third sample was prepared by mixing equal volumes of 80 min photolyzed aliquot and unphotolyzed aliquots and produced NCs containing 1.0 e^-_{CB}/NC. Thus, samples 2 and 3 had close to the same number of e^-_{CB}/NC but were prepared by different paths. The three samples were each reacted with

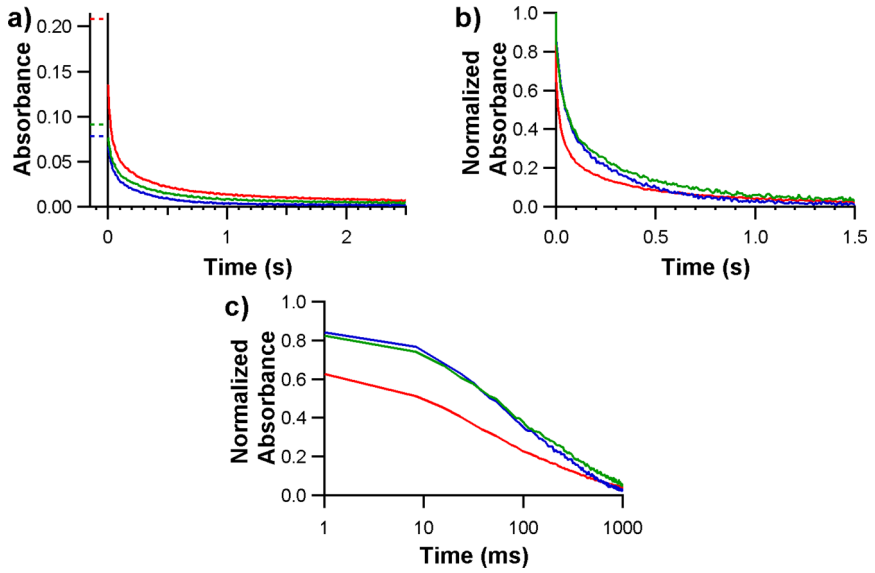

Figure 5. Kinetic plots for reactions of TEMPO (4.8 mM) with ZnO NCs ([NC] = 0.13 mM) reduced through different methods: 80 min photolysis (red), [e^-] = 0.30 mM; 80 min photolysis then diluted with unphotolyzed NCs (blue), [e^-] = 0.11 mM; 80 min photolysis then prereaction in the glovebox with a small amount of TEMPO (green), [e^-] = 0.13 mM). (a) A(700) *vs t*. (b) Normalized absorbance $(A_t - A_{final})/(A_{initial} - A_{final})$ *vs t*. The dashed lines before zero indicate the expected initial absorbance for each NC aliquot if no reaction occurred, obtained from half of the absorbance of a spectrum of reduced, unreacted NCs in the stopped-flow. (c) Normalized absorbance data plotted on a semilog scale.

the same 4.8 mM TEMPO solution. Plots of absorbance and normalized absorbance $(A_t - A_{final})/(A_{initial} - A_{final})$ *vs* time are shown in Figure 4. The normalized absorbance plot shows that the more reduced NCs react faster than the less reduced NCs, as observed previously. For the NCs prepared by short photolysis and by dilution, both the absorbance and normalized absorbance traces nearly overlay. Thus, the two samples of NCs with similar ~1 e^-_{CB}/NC, formed by different procedures, have similar reaction dynamics with TEMPO.

To extend the previous analysis of NC reactivity dependence on the path to reduction, the experiments described in Scheme 1c were performed. An 80 min photolyzed sample had 2.3 e^-_{CB}/NC once loaded onto the stopped-flow instrument. An aliquot of this sample diluted with the unphotolyzed solution yielded NCs with 0.8 e^-_{CB}/NC. The last portion was titrated in the glovebox with a substoichiometric amount of TEMPO to produce a solution with 1.0 e^-_{CB}/NC on average. All of the solutions were reacted with the same concentration of TEMPO in greater than 10-fold excess. The resulting plot of absorbance at 700 nm *vs* time appears similar to those shown above (Figure 5a). The normalized and semilog kinetic traces (Figure 5b,c) show that the most reduced aliquot reacts fastest, as expected. For the two less reduced samples, the TEMPO-quenched sample initially reacts slightly faster, as expected because it has a slightly higher [e^-]. In the second half of the reaction, however, the traces for these two samples diverge. The reaction velocity of the sample prereacted with TEMPO is *lower* than the diluted sample, even though it had a slightly *higher* initial electron concentration. These two samples have different reactivity, even though they have essentially the same concentration of electrons. They have just had a different path to get to that [e^-].

There is another way to look at these data to further probe whether the pathway to a certain concentration of electrons is important. Consider the reactions of the most highly charged NCs, those that had been irradiated for 80 min and have ca. 2.5 e^-_{CB}/NC. When these react with TEMPO in the stopped flow instrument, after about 30−50 ms they reach ~1 e^-_{CB}/NC. This is the same concentration as the less photolyzed, diluted, or preoxidized samples. However, this ~1 e^-_{CB}/NC sample has a quite different kinetic behavior with the same amount of TEMPO. The best way to illustrate this is to adjust the time axis of the *A*(700) *vs* time trace of the more highly reduced sample, so that it has the same absorbance as the less-reduced sample at "*t* = 0". Conceptually, this is like treating the first 30−52 ms of the reaction as a "pre-reaction" to prepare a sample with ~1 e^-_{CB}/NC. Figure 6a shows this "time axis-shifted" plot for the data in Figure 4. Upon shifting the time axis of the 80 min photolysis NC sample to the initial absorbance of the 20 min photolysis NCs, it is observed that the absorption for the 20 min photolyzed NCs decays more quickly than NCs that initially were more reduced. The 20 min photolyzed sample is significantly more reactive than the 80 min sample that has reached ~1 e^-_{CB}/NC in the stopped-flow. The same behavior is seen when the data from Figure 5 are time shifted (Figure 6b ,c): the initially more reduced sample is less reactive once it reaches the lower charging level inside the stopped-flow.

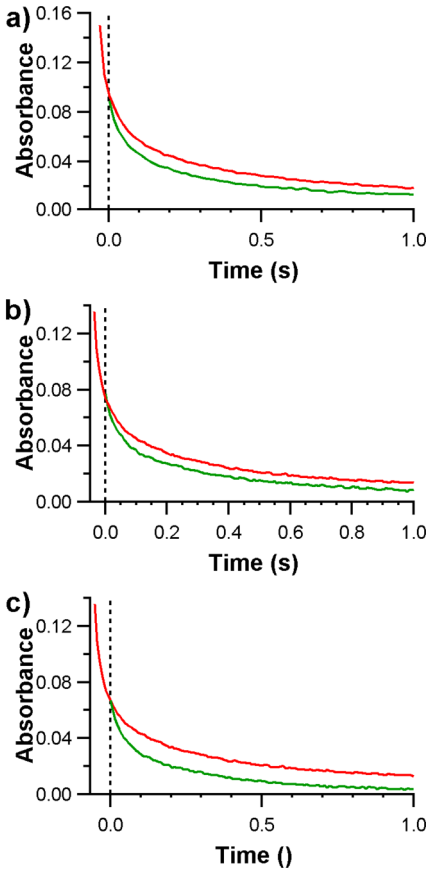

Figure 6. Kinetic plots for reactions of TEMPO with ZnO NCs in which the time axis for the red data has been shifted to the left so that at it has the same absorbance as the other sample at t = "0" (indicated by the vertical dotted line). (a) Data from Figure 4, with the 80 min photolyzed sample (initially 2.6 e^-_{CB}/NC, red) shifted 30 ms to the left to overlap with the 20 min photolyzed data (initially 1.1 e^-_{CB}/NC, green). (b) Data from Figure 5, with the 80 min photolyzed sample (initially 2.3 e^-_{CB}/NC, red) shifted 45 ms to the left to overlap with the TEMPO-prereacted sample (initially 1.0 e^-_{CB}/NC, green). (c) Data from Figure 5, with the 80 min photolyzed sample (initially 2.3 e^-_{CB}/NC, red) shifted 52 ms to the left to overlap with the diluted sample (initially 0.8 e^-_{CB}/NC, green).

These various examples show that NC aliquots with the same concentration of electrons can have different reactivity if they are prepared by different paths. These comparisons are made on the same batch of photoreduced NCs, so the compared suspensions have the same concentration and the same distribution of sizes, shapes, capping groups, and protons. This is one of the most important conclusions of this study; the reactivity of otherwise identical NCs does not simply scale with the concentration of electrons. This conclusion contrasts with the implicit assumptions in Gerischer-type models typically used for semiconductor–solution charge-transfer reactions.[21,22] These models emphasize the energy of the electrons or holes (typically the Fermi energy).

E. Mechanistic Overview of Proton-Coupled Electron Transfer at Colloidal ZnO Nanocrystals. The reaction of photoreduced ZnO (ZnO:e^-_{CB}/H^+) with the nitroxyl radical TEMPO (eq 1) is a proton-coupled electron-transfer process because both e^- and H^+ are transferred to form TEMPO-H. Reaction 1 has been studied by traditional stopped-flow mixing kinetics, appropriate for its time scale of milliseconds to seconds. The two reagents start in different solutions and undergo many collisions prior to reaction. (The collision frequency under these conditions is $>10^8$ s^{-1}; see the Supporting Information.) These reactions are therefore somewhat different than the more traditional studies of photoinitiated processes, which occur on much shorter time scales and often involve precoordinated substrates (*cf.* ref 23).

The kinetics of reaction 1 being first order in [TEMPO] is similar to the first-order dependence of the reaction of ZnO:e^-_{CB}/H^+ with the phenoxyl radical $^tBu_3ArO^\bullet$ observed in our previous laser-flash photolysis study.[11] The precise details of how TEMPO approaches the surface and acquires the e^- and H^+ are not known. The density of dodecylamine (DDA) capping ligands on these NCs is relatively low (~25–50%),[24] so the surface is accessible to the TEMPO. To avoid the effects of changes in capping ligand density, all of the comparative experiments described here involved solutions with the same DDA/NC ratio. The reaction must occur at a particular site on the surface because a proton is a quite localized particle, able to tunnel only a few tenths of an angstrom.[25] Reaction 1 is very unlikely to occur by initial outer-sphere electron transfer because TEMPO has a very negative redox potential even in polar media, and formation of the $TEMPO^-$ anion in the nonpolar toluene is very unfavorable.[26] Similarly, TEMPO is not a strong base, and the NC acidity is buffered by the excess DDA present, so initial proton transfer to form $TEMPOH^{+\bullet}$ is also very unfavorable. It could be that TEMPO abstracts e^- and H^+ from a NC in one kinetic step, which would resemble a hydrogen atom transfer process (also termed concerted proton–electron transfer, CPET).[27] Alternatively, TEMPO could potentially bind to the surface, concomitant with transfer of an electron to form a $TEMPO^-$ ligand to a Lewis acidic zinc site, followed by protonation to form TEMPO-H. In either case, the proton must be at or very near the surface, likely present as a surface hydroxide or a surface-bound dodecylammonium ion ($C_{12}H_{25}NH_3^+$). Preliminary experiments with added strong base suggest the presence of at least dozens of surface protons in the nonreduced NC.[24] This is not surprising since the NCs are prepared hydrolytically and are not calcined. Photochemical charging adds a stoichiometric proton for each added electron.[11] The reduced NCs may have some protons intercalated into the ZnO, as there is strong evidence for intercalated e^- and H^+ in bulk ZnO.[28–31] Protons below the surface of a NC would have to diffuse to the surface to be reactive.

F. Multiexponential (Distributed) Kinetics. The reaction of ZnO:e^-_{CB}/H^+ + TEMPO (eq 1) is not first order in the

concentration of electrons. Reactions were monitored by the change in absorbance at 700 nm, which measures the decrease in the concentration of electrons, the limiting reagent in the experiments. The multiexponential behavior is illustrated by the contrast between the substantial amount of reaction within the 1 ms mixing time of the stopped-flow instrument *vs* the *ca*. 1 s needed for substantial completion. In reactions of NC suspensions with $>2e^-$/NC on average, $\sim$ 30% of the reaction is complete in the 1 ms mixing time while ca. 500 ms is needed to reach $\sim$90% of reaction.

Some of the multiexponential behavior could be due to the distribution of electrons within the ensembles of NCs, some having $1e^-$, some $2e^-$, *etc*. However, similar kinetics are observed even for samples with an average of 0.4 e^-/NC, in which the distribution is likely much narrower than in the $>2e^-$/NC samples. The added electrons have been shown to occupy conduction band states rather than trap states, even at 4 K.[13] The reduced NCs are stable for extended periods and do not form H_2. Control experiments mixing TEMPO with nonreduced ZnO NCs and mixing TEMPOH with reduced NCs showed no reaction. Thus, there are no indications of side reactions, for instance, with the DDA capping ligands. Addition of TEMPOH did not inhibit a reaction of ZnO:e^-_{CB}/H^+ + TEMPO, so there is no evidence for TEMPOH blocking reactive sites. Such blocking seems quite unlikely as the reactions only involve 0.4−3 TEMPO molecules per NC and there are hundreds of surface zinc ions and likely many dozens of surface protons.

Multiexponential or "distributed" kinetic behavior is often observed for CT reactions between molecules and nanomaterials. The most studied class are charge injection and back-electron transfer between semiconductors and surface-attached dyes. These are typically thought to be multiexponential because of a variety of dye/semiconductor structures and interactions.[32,33] The behavior of the injected electrons in nanoscale TiO_2 electrodes has also been interpreted with continuous-time random walk models of electron-hopping and -trapping events.[35] The complex kinetics of ET from WO_x nanorods to a soluble Fe(III) oxidant was ascribed to the varying energetics of the multiple electrons being transferred.[7]

It is not evident why the ZnO:e^-_{CB}/H^+ + TEMPO reaction has multiexponential kinetic behavior. However, there are a number of features of this reaction that constrain the possible explanations, starting with the slow rate of reaction and the simple first-order dependence on [TEMPO]. Consider first a hypothetical ensemble of *identical* ZnO:e^-_{CB}/H^+ particles with multiple reactive sites on the surface, perhaps multiple proton sites. This would not give multiexponential kinetic behavior. The reactions studied here are in the limit of many collisions per reactive event so that all surface sites will be explored. Identical ZnO:e^-_{CB}/H^+ particles with multiple reactive hydrogens on the surface would behave just like molecules in a solution, which might have, for instance, multiple reactive hydrogens. In propane ($CH_3CH_2CH_3$), for example, the primary and secondary hydrogen sites have different reactivities but that does not lead to multiexponential kinetics.[34]

The multiexponential kinetics therefore must result from some sort of heterogeneity of the NCs, a difference among the particles that is not rapidly equilibrating on the ms time scale. This heterogeneity could be in the sizes of the NCs, the energetics of the CB electrons, the faceting of the NCs, the number or position of the capping ligands, and the number and nature of the proton sites. We note that spectroscopic studies have shown that the added electrons in such ZnO NCs occupy orbitals that are delocalized over the entire NC.[13] Therefore, there is not the broad distribution of midgap electron trap states that are common in TiO_2 and other materials.

The uncharged ZnO NCs have a size distribution of about $\pm$17% about the mean, estimated from the shape of the band edge absorption.[36] This distribution of sizes leads to a distribution of electron energies in the NCs. It is important to note that electron transfer between NCs is rapid under these conditions. ET from smaller NCs to larger ones occurs within 2 ms even at 50 μM NCs.[20] Thus, as the reaction proceeds, the highest energy more reactive electrons should be depleted, and this could be the cause of the multiexponential kinetics. The results in Figure 3b support the qualitative prediction of this "electron energy" model, as the decay of the e^-_{CB} signal at 700 nm upon reaction with TEMPO is progressively slower in NCs with decreasing electron content. However, this model is not consistent with the conclusions of the previous section that the kinetic behavior is not just due to the number of electrons. The failure of this model can also been seen from the data in Figure 3, comparing the reactions of 2.7, 0.9, and 0.4 e^-_{CB}/NC samples. The last 15% of the reaction of the 2.7 e^-_{CB}/NC sample is dramatically slower than the initial reaction of the 0.4 e^-_{CB}/NC sample, even though they have the same electron concentration. Furthermore, electron transfer between PbS NCs and quinones with similar size distributions display single exponential kinetic behavior in the miscrosecond, collisional time frame.[23]

Thus, we conclude both that the NCs in the suspension must be inhomogeneous to account for the multiexponential kinetics, and that the electron concentration alone does not account for this heterogeneity. This is not a small effect, as rough fitting of the data to a biexponential model gives time constants for the fast and slow components that differ by an order of magnitude. It seems unlikely that this is due to variations in the size and shape of the NCs, given the

fairly narrow size distribution (±17%).[36] Similarly, heterogeneity in the capping group number and density seems unlikely to cause this large a variation given the low number of strongly bound groups.[12]

One possible explanation is that the effects observed here are related to the protons transferred in this PCET process. Perhaps there are different populations of protons compensating for the charge of the CB electrons, and these have varying abilities to transfer to TEMPO. The changes in the particles with time or different treatments could then relate to these proton populations. These NCs undoubtedly have surface protons in the form of surface hydroxyl groups from their hydrolytic synthesis and from the photoreduction process.[24,11] There is also a body of experimental[37,38] and computational[39] evidence for protons intercalating into bulk ZnO. The diffusivity of deuterium in bulk ZnO and ZnO films is likely ≥ 10 nm^2 s^{-1} (as extrapolated from higher temperature measurements[40,41]), so movement of protons in these NCs on this time scale is reasonable. The experiments reported here may perhaps be plausibly interpreted as more reactive surface protons being removed from the NC first and other protons having to migrate to those more reactive sites. The differences in reactivity observed between the samples partially oxidized with TEMPO versus partially oxidized with uncharged NCs could be due to these reagents removing protons from ZnO:e^-_{CB}/H$^+$ NCs in different ways.

The ZnO:e^-_{CB}/H$^+$ + TEMPO PCET reaction seems slow compared to related studies of ET reactions of nanocrystals.[20] Bimolecular ET from photoreduced PbS NCs to benzoquinone, for instance, occurs on the microsecond time scale (*e.g.*, $k_q = 4.7 \times 10^8$ M^{-1} s^{-1}).[42,23] Quantitative comparisons are difficult due to reaction 1 being multiexponential and showing substantial reactivity within the ca. 1 ms mixing time of the stopped-flow instrument, but the time scales of the reactions indicate bimolecular rate constants from 10 to 10^4 M^{-1} s^{-1} (see the Supporting Information). These are not atypical of molecular PCET reactions of TEMPO, which is fairly sterically crowded. More detailed interpretations of the reaction time scales will require as yet unavailable information about the free energies of the reactions. The slowness of the reactions described here does not appear to be simply due to their being PCET processes, as flash-kinetics experiments indicated rate constants of ca. 10^7 M^{-1} s^{-1} for the PCET reaction between the photoinduced reactions of ZnO NCs and ^{t}Bu$_3$ArO$^\bullet$.[11] ^{t}Bu$_3$ArO$^\bullet$ reactions are 0.46 eV more exoergic than analogous TEMPO reactions on the basis of their O−H bond dissociation free energies.[26]

CONCLUSIONS AND IMPLICATIONS

Proton-coupled electron transfer (PCET) from photoreduced colloidal ZnO nanocrystals (ZnO:e^-_{CB}/H$^+$ NCs) to the nitroxyl radical TEMPO proceeds over the millisecond to second time scale. The kinetics are first order in TEMPO. More highly reduced NCs react faster. The rate of decay of the electron concentration is multiexponential for all NCs, even those with less than 1e^-/NC on average. The multiexponential kinetic behavior is indicated to be due to the heterogeneity of the nanocrystals. We tentatively suggest that this heterogeneity is at least in part due to a distribution of the nature of the reactive protons. Reduced NCs from the same batch with the same average number of electrons per NC can have different kinetic behavior, depending on the different chemical routes to that electron concentration. For instance, two samples with the same average number of electrons per NC can be prepared from aliquots of a highly reduced ZnO:e^-_{CB}/H$^+$ NC suspension by partial oxidation with TEMPO or with uncharged ZnO NCs. Thus, the electronic composition and electron energy are not the sole determinant of reactivity. These results indicate limitations of the simple energy level diagrams which are commonly used to interpret interfacial redox reactivity. Future studies will probe whether these conclusions are general to PCET reactions of other oxides, to catalytic processes that involve PCET, or to reactions that involve just the transfer of an electron or hole.

EXPERIMENTAL SECTION

A. General Considerations. ZnO NCs were prepared as previously described[43] from the addition of ethanolic tetramethylammonium hydroxide to zinc acetate in dimethyl sulfoxide/ethanol at 0 °C. The NCs were washed with ethanol twice and capped with dodecylamine before being suspended in toluene. These stock solutions of NCs were bubble degassed under reduced pressure and stored at −35 °C in an N_2-filled glovebox. The ZnO NC concentrations were calculated from the average NC size (4 to 4.2 nm in diameter), determined from optical spectra of dilute solutions,[44] together with the zinc concentration of those solutions, measured by ICP-AES. TEMPO (Sigma-Aldrich) was sublimed before use. Dodecylamine, 98% from Sigma-Aldrich, was used without further purification. Toluene was obtained from a Seca Solvent System installed by GlassContour.

Manipulations of solutions were completed in an air-free glovebox, unless otherwise noted. In a typical experiment, a ZnO NC stock solution was removed from cold storage and allowed to reach room temperature, 24 ± 1 °C. An experimental solution of 0.26−0.34 mM ZnO NC was prepared by dilution with toluene. Photoreduction of the experimental solutions was achieved by removing a portion of this solution from the glovebox in a quartz reaction vessel outfitted with a Kontes valve and a Teflon coated stir-bar, followed by photolysis for 20 to 80 min with stirring using an Oriel 200 W Hg/Xe arc lamp (Model 66056) and power supply (Model 68742, operating at 6 A). After the desired photolysis time, the reduced NC solution was returned to the glovebox and split into aliquots which were further manipulated, vide infra. These aliquots were loaded into 5 or 10 mL gastight syringes with valves. Gastight syringes of degassed toluene and solutions of TEMPO were also prepared in the glovebox.

The NC aliquots, solvent, and reagent-filled syringes were removed from the glovebox and attached to the sample

handling unit of a TgK Double-Mixing Cryo Stopped-Flow Instrument. Hamilton "T"-valves were attached between the sample and reservoir syringes to aid in removing air bubbles. The reservoir syringes and reagent lines were rinsed with 3−4 mL of degassed solvent before being replaced with syringes of reduced NC or TEMPO solutions. Spectra to determine the [e^-] were obtained by pushing 0.5−1.5 mL of the NC solution through the observation cell prior to and after reactions. The actual initial reaction concentrations were half of this measured value (to account for mixing with the TEMPO solution) and are indicated by dashed lines in many of the figures. Reactions were performed at 0 °C and monitored between 340 and 705 nm with the diode array detector. Data were collected from the mixing time of the instrument, ca. 1 ms, over time courses of 1.5−35 s depending on the conditions, using integration times of 1.5−2 ms.

PCET from reduced ZnO NCs to TEMPO was monitored through the loss of a broad absorbance in the visible spectrum of the reaction solution. This visible absorbance is the high energy tail of a very broad band peaking in the IR and has been described as an intraband absorption of the CB electrons.[45] While the shape and intensity of this overall resonance is a complex function of the concentration of electrons, we have shown by titration that for these sizes of NCS, the absorbance at 700 nm is a linear function of the number of electrons, with an extinction coefficient $\varepsilon = 700 \pm 100\ M^{-1}\ cm^{-1}$.[12] This ε and the spectra mentioned above determined the electron concentration of the NC suspension. While there is some small variation in the ε from one experiment to another, in every case the absorbance at 700 nm depends linearly on the [e^-] based on titration experiments. Therefore, the kinetics of the reactions were analyzed using the absorbance at 700 nm.

B. Manipulation of Experimental NC Samples. The electron content of the NC samples was modulated in three different ways; changing photolysis time, dilution with unreduced NCs, and oxidation with TEMPO (Scheme 1). This allowed us to observe how the path to a particular electron concentration affected the reaction of the NCs with TEMPO.

One set of experiments to probe the effect of electron concentration is illustrated in Scheme 1a (results in Figure 3). An experimental solution was prepared by diluting 15 mL of a stock solution to 20 mL ([NC] = 0.26 mM) with toluene. A 12 mL portion was transferred to the gastight quartz vessel photolyzed for 80 min. Three aliquots were prepared for comparison on the stopped-flow spectrometer: 7 mL of the photolyzed experimental solution, 3 mL of the photolyzed solution mixed with an equal volume of the unphotolyzed solution, and 1.5 mL of the photolyzed solution mixed with 4 mL of the unphotolyzed solution. Previous work has shown that inter-NC ET is fast and should rapidly equilibrate the electrons across all the NCs in the colloidal suspension.[20] This kind of procedure was followed in all of the experiments reported here to ensure that the NC properties were identical for all of the kinetic runs within a comparative set. This avoids the incidental variation in the properties of the NCs between synthetic batches, for instance, in the concentration of dodecylamine capping groups. For example, the dilution experiments mixed reduced NCs with unphotolyzed NCs from the same batch, thus maintaining a constant capping ligand/NC ratio.

In order to probe whether the pathway to NC electron content has an effect on the reaction with TEMPO, the experiments in Scheme 1b were undertaken (results in Figure 4). An experimental solution was prepared by diluting 15 mL of a stock solution to 20 mL ([NC] = 0.26 mM) with toluene. This solution was separated into three aliquots of 10, 6, and 4 mL. The 10 and 6 mL aliquots were photolyzed for 80 and 20 min, respectively, and the 4 mL aliquot was left unphotolyzed. A 3 mL portion of the 80 min photolyzed aliquot was mixed an equal volume of the unphotolyzed aliquot.

The experiments illustrated in Scheme 1c (Figure 5) used a 20 mL experimental solution, prepared as described above, separated into 16 and 4 mL aliquots. The 16 mL aliquot was photolyzed for 80 min. A 6 mL portion of the photolyzed solution was oxidized with a 110 μL volume of TEMPO (19.2 mM), monitoring this reaction with an Ocean Optics UV−vis spectrometer in the glovebox. A 3 mL portion of the photolyzed sample was diluted with an equal volume of the photolyzed aliquot. A 7 mL portion of the photolyzed aliquot was kept for comparison with the other two samples.

Conflict of Interest: The authors declare no competing financial interest.

Supporting Information Available: The Supporting Information is available free of charge on the ACS Publications website at DOI: 10.1021/acsnano.5b04222.

Data analysis and plots using double-exponential and stretched exponential fits; normalized absorbance *vs* log(time) plots; estimation of the diffusion limited rate constants for nanoparticle reactions (PDF)

Acknowledgment. We gratefully acknowledge primary support from the U.S. National Science Foundation (CHE-1151726), with initial support from the donors of the American Chemical Society Petroleum Research Fund (51178-ND3) and the University of Washington and with partial support from Yale University. We thank Dr. B. McKeown for related experiments and C. N. Valdez for valuable discussions.

REFERENCES AND NOTES

1. Walter, M. G.; Warren, E. L.; McKone, J. R.; Boettcher, S. W.; Mi, Q.; Santori, E. A.; Lewis, N. S. Solar Water Splitting Cells. *Chem. Rev.* **2010**, *110*, 6446–6473.
2. Nozik, A. J. Photoelectrochemistry: Applications to Solar Energy Conversion. *Annu. Rev. Phys. Chem.* **1978**, *29*, 189–222.
3. Viswanathan, B., Subramanian, V., Lee, J. S., Eds. *Materials and Processes for Solar Fuel Production*; Springer, 2014; Vol. 174.
4. Berger, T.; Monllor-Satoca, D.; Jankulovska, M.; Lana-Villarreal, T.; Gomez, R. The Electrochemistry of Nanostructured Titanium Dioxide Electrodes. *ChemPhysChem* **2012**, *13*, 2824–2875.
5. Bard, A. J. Inner-Sphere Heterogeneous Electrode Reactions. Electrocatalysis and Photocatalysis: The Challenge. *J. Am. Chem. Soc.* **2010**, *132*, 7559–7567.
6. Knowles, K. E.; Frederick, M. T.; Tice, D. B.; Morris-Cohen, A. J.; Weiss, E. A. Colloidal Quantum Dots: Think Outside the (Particle-in-a-)Box. *J. Phys. Chem. Lett.* **2012**, *3*, 18–26.
7. Grauer, D. C.; Alivisatos, A. P. Ligand Dissociation Mediated Charge Transfer Observed at Colloidal $W_{18}O_{49}$ Nanoparticle Interfaces. *Langmuir* **2014**, *30*, 2325–2328.
8. Liu, G.; Yu, J. C.; Lu, G. Q.; Cheng, H. Crystal Facet Engineering of Semiconductor Photocatalysts: Motivations, Advances and Unique Properties. *Chem. Commun.* **2011**, *47*, 6763–6783.
9. Hamann, T. W.; Gstrein, F.; Brunschwig, B. S.; Lewis, N. S. Measurement of the Free-Energy Dependence of Interfacial Charge-Transfer Rate Constants using ZnO/H_2O Semiconductor/Liquid Contacts. *J. Am. Chem. Soc.* **2005**, *127*, 7815–7824.
10. Lyon, A. L.; Hupp, J. T. Energetics of the Nanocrystalline Titanium Dioxide/Aqueous Solution Interface: Approximate Conduction Band Edge Variations between $H_0 = -10$ and $H_- = +26$. *J. Phys. Chem. B* **1999**, *103*, 4623–4628.
11. Schrauben, J. N.; Hayoun, R.; Valdez, C. N.; Braten, M.; Fridley, L.; Mayer, J. M. Titanium and Zinc Oxide Nanoparticles are Proton-Coupled Electron Transfer Agents. *Science* **2012**, *336*, 1298–1301.
12. Valdez, C. N.; Braten, M.; Soria, A.; Gamelin, D. R.; Mayer, J. M. Effect of Protons on the Redox Chemistry of Colloidal Zinc Oxide Nanocrystals. *J. Am. Chem. Soc.* **2013**, *135*, 8492–8495.
13. Whitaker, K. M.; Ochsenbein, S. T.; Polinger, V. Z.; Gamelin, D. R. Electron Confinement Effects in the EPR Spectra of Colloidal n-Type ZnO Quantum Dots. *J. Phys. Chem. C* **2008**, *112*, 14331–14335.
14. Haase, M.; Weller, H.; Henglein, A. Photochemistry and Radiation Chemistry of Colloidal Semiconductors. 23.

Electron Storage on Zinc Oxide Particles and Size Quantization. *J. Phys. Chem.* **1988**, *92*, 482–487.
15. Shim, M.; Guyot-Sionnest, P. Organic-Capped ZnO Nanocrystals: Synthesis and n-Type Character. *J. Am. Chem. Soc.* **2001**, *123*, 11651–11654.
16. Mohamed, H. H.; Mendive, C. B.; Dillert, R.; Bahnemann, D. W. Kinetic and Mechanistic Investigations of Multielectron Transfer Reactions Induced by Stored Electrons in TiO_2 Nanoparticles: A Stopped Flow Study. *J. Phys. Chem. A* **2011**, *115*, 2139–2147.
17. Jiao, F.; Frei, H. Nanostructured Cobalt and Manganese Oxide Clusters as Efficient Water Oxidation Catalysts. *Energy Environ. Sci.* **2010**, *3*, 1018–1027.
18. Look, J. L.; Wick, D. D.; Mayer, J. M.; Goldberg, K. I. Autoxidation of Platinum(IV) Hydrocarbyl Hydride Complexes To Form Platinum(IV) Hydrocarbyl Hydroperoxide Complexes. *Inorg. Chem.* **2009**, *48*, 1356–1369.
19. A rate law that is first-order in [TEMPO] can be written as $d[e^-]/dt = f([e^-])[\text{TEMPO}]$, where the $f([e^-])$ term describes the nonexponential form of the kinetics and is independent of [TEMPO]. Rearranging to $d[e^-] = f([e^-])\{[\text{TEMPO}]dt\}$ shows that the reaction course should be invariant to the product of [TEMPO] times time under conditions of excess (constant) [TEMPO].
20. Hayoun, R.; Whitaker, K. M.; Gamelin, D. R.; Mayer, J. M. Electron Transfer Between Colloidal ZnO Nanocrystals. *J. Am. Chem. Soc.* **2011**, *133*, 4228–4231.
21. Koval, C. A.; Howard, J. N. Electron Transfer at Semiconductor Electrode-Liquid Electrolyte Interfaces. *Chem. Rev.* **1992**, *92*, 411–433.
22. Morrison, S. R. *Electrochemistry at Semiconductor and Oxidized Metal Electrodes*; Springer, 1988.
23. Knowles, K. E.; Tagliazucchi, M.; Malicki, M.; Swenson, N. K.; Weiss, E. A. Electron Transfer as a Probe of the Permeability of Organic Monolayers on the Surfaces of Colloidal PbS Quantum Dots. *J. Phys. Chem. C* **2013**, *117*, 15849–15857.
24. Valdez, C. N.; Schimpf, A. M.; Gamelin, D. R.; Mayer, J. M. Low Capping Group Surface Density on Zinc Oxide Nanocrystals. *ACS Nano* **2014**, *8*, 9463–9470.
25. Krishtalik, L. I. The Mechanism of the Proton Transfer: An Outline. *Biochim. Biophys. Acta, Bioenerg.* **2000**, *1458*, 6–27.
26. Warren, J. J.; Tronic, T. A.; Mayer, J. M. Thermochemistry of Proton-Coupled Electron Transfer Reagents and its Implications. *Chem. Rev.* **2010**, *110*, 6961–7001.
27. Mayer, J. M. Understanding Hydrogen Atom Transfer: From Bond Strengths to Marcus Theory. *Acc. Chem. Res.* **2011**, *44*, 36–46.
28. Van de Walle, C. G. Hydrogen as a Cause of Doping in Zinc Oxide. *Phys. Rev. Lett.* **2000**, *85*, 1012–1015.
29. Cox, S. F. J.; Davis, E. A.; Cottrell, S. P.; King, P. J. C.; Lord, J. S.; Gil, J. M.; Alberto, H. V.; Vilão, R. C.; Piroto Duarte, J.; Ayres de Campos, N.; et al. Experimental Confirmation of the Predicted Shallow Donor Hydrogen State in Zinc Oxide. *Phys. Rev. Lett.* **2001**, *86*, 2601–2604.
30. Lavrov, E. V.; Herklotz, F.; Weber, J. Identification of Two Hydrogen Donors in ZnO. *Phys. Rev. B: Condens. Matter Mater. Phys.* **2009**, *79*, 165210.
31. Shi, G. A.; Stavola, M.; Pearton, S. J.; Thieme, M.; Lavrov, E. V.; Weber, J. Hydrogen Local Modes and Shallow Donors in ZnO. *Phys. Rev. B: Condens. Matter Mater. Phys.* **2005**, *72*, 195211.
32. Anderson, N. A.; Tianquan, L. Ultrafast Electron Transfer at the Molecule-Semiconductor Nanoparticle Interface. *Annu. Rev. Phys. Chem.* **2005**, *56*, 491–519.
33. Wong, N. A.; Ogata, A. F.; Wustholz, K. L. Dispersive Electron-Transfer Kinetics from Single Molecules on TiO_2 Nanoparticle Films. *J. Phys. Chem. C* **2013**, *117*, 21075–21085.
34. For hydrogen abstraction (PCET) from propane by a radical $X^\bullet$, $d[CH_3CH_2CH_3]/dt = \{2k_{2^\circ(CH_3CH_2CH_3)} + 6k_{1^\circ(CH_3CH_2CH_3)}\}[CH_3CH_2CH_3][X^\bullet]$ (the numbers reflecting the statistical weight of the different Hs). This is a simple second-order rate law that will give exponential decay of propane in the presence of excess $X^\bullet$ (the conditions used here for eq 1).
35. Ardo, S.; Meyer, G. J. Photodriven Heterogeneous Charge Transfer with Transition-Metal Compounds Anchored to TiO_2 Semiconductor Surfaces. *Chem. Soc. Rev.* **2009**, *38*, 115–164.
36. Pesika, N. S.; Stebe, K. J.; Searson, P. C. Relationship between Absorbance Spectra and Particle Size Distributions for Quantum-Sized Nanocrystals. *J. Phys. Chem. B* **2003**, *107*, 10412–10415.
37. Kohiki, S.; Nishitani, M.; Wada, T.; Hirao, T. Enhanced Conductivity of Zinc Oxide Thin Films by Ion Implantation of Hydrogen. *Appl. Phys. Lett.* **1994**, *64*, 2876–2878.
38. Chianella, C.; Palombari, R.; Petricca, A. Electrochemical Hydrogen Doping of Zinc Oxide: A Study of the Oxide–Proton Conductor Interface. *Electrochim. Acta* **2006**, *52*, 369–372.
39. Janotti, A.; Van De Walle, C. G. Fundamentals of Zinc Oxide as a Semiconductor. *Rep. Prog. Phys.* **2009**, *72*, 126501–126530.
40. Nickel, N. H. Hydrogen Migration in Single Crystal and Polycrystalline Zinc Oxide. *Phys. Rev. B: Condens. Matter Mater. Phys.* **2006**, *73*, 195204.
41. Ip, K.; Overberg, M. E.; Heo, Y. W.; Norton, D. P.; Pearton, S. J.; Stutz, C. E.; Luo, B.; Ren, F.; Look, D. C.; Zavada, J. M. Hydrogen Incorporation and Diffusivity in Plasma-Exposed Bulk ZnO. *Appl. Phys. Lett.* **2003**, *82*, 385–387.
42. Knowles, K. E.; Malicki, M.; Weiss, E. A. Dual-Time Scale Photoinduced Electron Transfer from PbS Quantum Dots to a Molecular Acceptor. *J. Am. Chem. Soc.* **2012**, *134*, 12470–12473.
43. Norberg, N. S.; Gamelin, D. R. Influence of Surface Modification on the Luminescence of Colloidal ZnO Nanocrystals. *J. Phys. Chem. B* **2005**, *109*, 20810–20816.
44. Meulenkamp, E. A. Synthesis and Growth of ZnO Nanoparticles. *J. Phys. Chem. B* **1998**, *102*, 5566–5572.
45. Schimpf, A. N.; Thakkar, N.; Gunthardt, C. E.; Masiello, D. J.; Gamelin, D. R. Charge-Tunable Quantum Plasmons in Colloidal Semiconductor Nanocrystals. *ACS Nano* **2014**, *8*, 1065–1072.